

DOI: 10.1002/adma.200702956

# Individual Water-Filled Single-Walled Carbon Nanotubes as Hydroelectric Power Converters\*\*

By Yuanchun Zhao, Li Song, Ke Deng, Zheng Liu, Zengxing Zhang, Yanlian Yang, Chen Wang, Haifang Yang, Aizi Jin, Qiang Luo, Changzhi Gu, Sishen Xie,\* and Lianfeng Sun\*

The filling, structure, and transport properties of water confined in one-dimensional nanochannels are of great interest in physics, biology, and materials science.<sup>[1]</sup> An ideal model for these studies is water that is confined inside carbon nanotubes, specifically, single-walled carbon nanotubes (SWNTs). Molecular dynamic (MD) simulations predicted that water can enter the hydrophobic channels of SWNTs which gives rise to unique structures and transport behavior.<sup>[2]</sup> Experimental studies, including X-ray diffraction (XRD),<sup>[3]</sup> NMR spectroscopy,<sup>[4]</sup> neutron scattering,<sup>[5]</sup> IR spectroscopy,<sup>[6]</sup> and Raman spectroscopy,<sup>[7]</sup> demonstrated notable changes in properties that are induced by water (H<sub>2</sub>O/D<sub>2</sub>O) being encapsulated in open-ended SWNTs, which in turn confirmed that water can indeed occupy SWNT channels. Furthermore, water confined in closed multiwalled carbon nanotubes (MWNTs) of 2–5 nm diameter was directly observed using transmission electron microscopy (TEM).<sup>[8]</sup> Very recently, a remarkably enhanced transport of water through nanotube membranes was reported,<sup>[9]</sup> and the possibility of water-filled SWNTs being employed as nanovalves to control a gas flow inside SWNTs has been proposed.<sup>[10]</sup>

Water flowing inside/outside SWNTs represents a unique nanofluidic system, in which the water molecules and the walls of the SWNTs form an intimate contact on the atomic level.

[\*] Prof. L. Sun, Dr. Y. Zhao, Prof. K. Deng, Dr. Z. Liu, Prof. Y. Yang, Prof. C. Wang  
National Center for Nanoscience and Technology  
No. 11, Beiyitiao Zhongguancun, Beijing, 100080 (P.R. China)  
E-mail: slf@nanoctr.cn  
Prof. S. Xie, Dr. L. Song, Dr. Z. Zhang, Dr. H. Yang, Dr. A. Jin, Dr. Q. Luo, Prof. C. Gu  
Beijing National Laboratory of Condensed Matter Physics  
Institute of Physics  
Chinese Academy of Sciences  
P. O. Box 603, Beijing, 100080 (P.R. China)  
E-mail: sxxie@aphy.iphy.ac.cn  
Dr. Y. Zhao, Dr. Z. Liu  
Graduate School of the Chinese Academy of Sciences  
Beijing, 100049 (P.R. China)

[\*\*] This work was supported by the “100 Talents Program”, the Knowledge Innovation Program of the Chinese Academy of Sciences, the “973” Program of the Ministry of Science and Technology (2006CB932402), and the National Science Foundation of China. We thank Q. Xue, W. Guo, H. Gao, W. Zhou, C. Wang, G. Liu and W. Ma for helpful discussions. Supporting Information is available online from Wiley InterScience or from the authors.

Although, the transport of water through nanotube membranes was shown to be highly efficient,<sup>[9]</sup> it is not entirely frictionless. Due to the polar nature of the water molecules a weak coupling is observed between water dipoles and free charge carriers of the nanotubes.<sup>[11,12]</sup> Theoretical work of Král and Shapiro proposes that an electric current is generated along a metallic SWNT if it is immersed in a flowing liquid,<sup>[13]</sup> whereby the dominant mechanism is believed to be the momentum transfer process from the flowing liquid to the acoustic phonons, and from there to the free charge carriers in the nanotube. Ghosh et al.<sup>[12]</sup> showed experimentally that a voltage is induced by water and/or other polar/ionic fluids flowing over bundles of SWNTs. They reasoned that the free charge carriers present in the SWNTs are dragged along the nanotube by the fluctuating Coulomb field that is caused by a liquid flowing past the nanotubes. However, the weak interaction between water molecule and SWNT wall, which determines the transport behavior of water through the nanotube channels, still lacks a fundamental and clear understanding. It is quite possible that the coupling between water dipoles and free charge carriers in the nanotube is mutual, i.e., a constant current can induce a directional water flow inside the nanotube, whereby the one-dimensional confinement of the nanotube channel ensures that the induced water flow is steady and concerted, which is very much different to the water flow outside of the SWNT.

In this communication, we report on the detection of a significant voltage difference at one end of an individual nanotube of a SWNT device when a current is applied on the opposite side and it is exposed to water vapor. We suggest that a water flow is induced inside the SWNT which is driven by the applied current and causes one part of the device to act as a “motor”. Thereby electrical energy is partially converted into kinetic energy of the water molecules and the water flow subsequently generates an electromotive force along the other part of nanotube, the “generator” (Fig. 1b).

Individual SWNTs with an average diameter of ~1.6 nm were used to fabricate SWNT devices, whereby individual nanotubes were suspended ~100 nm above the substrate surface (Si wafer) to exclude possible effects of the SiO<sub>2</sub> layer. A focused ion beam (FIB) was used to open both ends of the SWNTs, thus allowing water molecules to fill the nanotube channels. Figure 1a shows a typical scanning electron microscopy (SEM) image of an as-fabricated SWNT device.

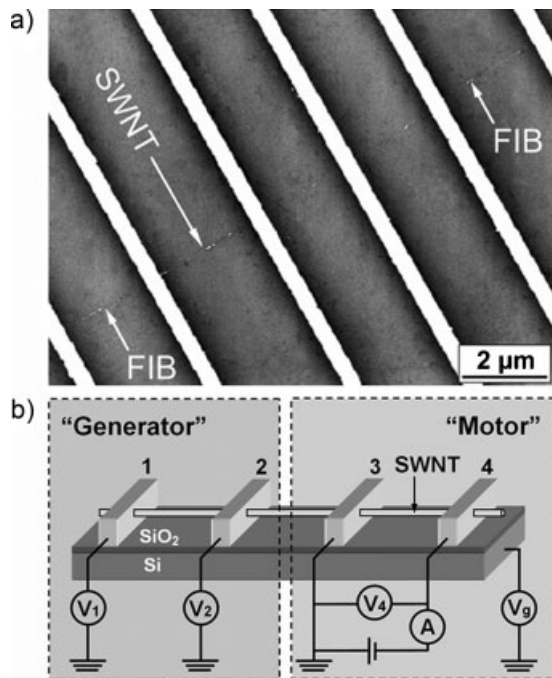


**Figure 1.** a) A typical scanning electron microscopy (SEM) image of an individual single walled carbon nanotube (SWNT) device prior to focused ion beam (FIB) cutting. b) Schematic device structure. A suspended SWNT is connected to four electrodes. Current/voltage is applied between electrodes 3 and 4 (“motor” part) and the induced electromotive force will result in a voltage difference being measured between electrodes 1 and 2 (“generator” part) when the device is exposed to water vapor.

Devices were loaded into a steel chamber (0.8 L), which was evacuated to approximately  $10^{-4}$  Pa, and measurements were performed using a modified four-probe contact configuration. As shown in Figure 1b, current/voltage was applied between electrodes 3 and 4 (“motor” part, electrode 3 was grounded), and two voltmeters were connected to electrodes 1 and 2 (“generator” part). All measurements were carried out at room temperature.

Firstly, we measured the  $I$ - $V$  characteristics of the device in vacuum. As displayed in Figure 2a, the voltages  $V_1$  and  $V_2$  are not zero due to the contact resistance between electrode 3 and nanotube (Fig. 2b,  $R_3$ ). Both,  $V_1$  and  $V_2$  are equal to the voltage at point “A” (Fig. 2b), because there is no current flowing in the SWNT on the left hand side of electrode 3 ( $I < 1$  pA). The  $I$ - $V$  characteristic of the “3–4” part of the nanotube shows linear

behavior (inset of Fig. 2a) and no dependence on the gate voltage, which indicates that the SWNT is metallic. Then, 600  $\mu$ L deionized water (MilliQ,  $18 \text{ M}\Omega \cdot \text{cm}^{-1}$ ) was injected into the chamber. To ensure the water molecules are uniformly dispersed in the chamber, the following measurements were performed several minutes later. Figure 2c shows the  $I$ - $V$  characteristics of the device when it is exposed to water vapor. Compared to the vacuum the absolute values of  $V_1$  and  $V_2$  are larger, but most importantly,  $V_1$  and  $V_2$  are no longer equal to each other, and thus a voltage difference ( $\Delta V = V_1 - V_2$ ) is measured in the “generator” part of the device. The induced  $\Delta V$  shows a linear dependence on the current applied on the “motor” part. This voltage difference reveals a newly induced electromotive force along the nanotube, which is directly related to the injection of water vapor into the chamber. It should be noted that similar voltage differences were measured in six other working devices (see Supporting Information).

When the device is exposed to water vapor the absorption of water molecules firstly changes the work function of the metal electrodes,<sup>[14]</sup> and then the contact resistance  $R_3$  (Fig. 2d,  $R_3'$ ), which in turn results in changes in  $V_1$  and  $V_2$ . The adsorbed water molecules also donate electrons to the nanotube through a charge transfer process,<sup>[15]</sup> which slightly changes the nanotube resistance ( $R_{NT}$ ). However, conventional changes in  $R_3$  and  $R_{NT}$  cannot generate the voltage difference measured between electrodes 1 and 2. Hence, the measured voltage difference must be generated by other mechanisms.

When water is injected into an evacuated chamber water molecules are uniformly dispersed. The collision rate,  $r_c$ , of

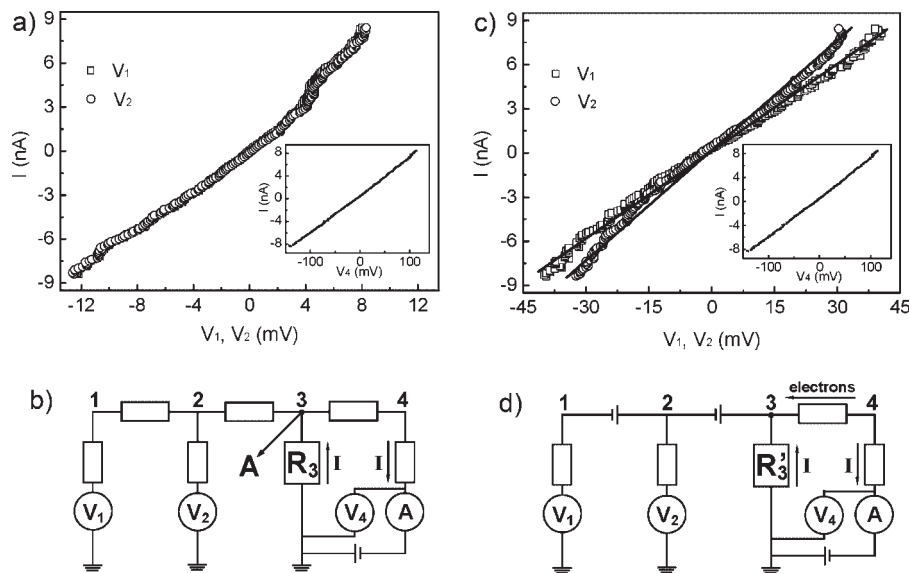


**Figure 2.** a) Under vacuum  $V_1$  and  $V_2$  are almost equal and show linear dependence on the current applied. The inset shows the linear  $I$ - $V$  characteristic of the device. b) Under vacuum  $V_1$  and  $V_2$  equal the voltage at point “A”. The contacts between electrodes and SWNT can be described by four contact resistors. c) If water vapor is present in the chamber a significant difference between  $V_1$  and  $V_2$  is observed. The inset confirms that the  $I$ - $V$  characteristic of the device is still linear. d) In the case of a negative current, the flowing water inside the SWNT can induce voltages in sections “1–2” and “2–3” of the SWNT, respectively. The voltage difference  $\Delta V$  ( $\Delta V = V_1 - V_2$ ) can eliminate changes in  $R_3$ .

water molecules with one open end of the SWNT (diameter  $\sim 1.6$  nm) can be estimated using Equation (1):

$$r_c = \frac{1}{4}nvS \quad (1)$$

where  $n$  is the density of water molecules in the chamber,  $v$  the velocity of water molecules, and  $S$  the area of the open end of the SWNT. Upon injection of  $600 \mu\text{L}$  water into the chamber the water molecule density is  $\sim 0.025$  water molecules per  $\text{nm}^3$ . At  $25^\circ\text{C}$  the velocity of water molecules is  $\sim 641 \text{ nm} \cdot \text{ns}^{-1}$ , thus about eight molecules collide with the open end per nanosecond. Previously published works predicted that SWNT channels possess a deep potential well in their interior, which is strong enough to break some of the hydrogen bonds of liquid water and suck single water molecules into nanotube channels.<sup>[2]</sup> And, if the water is already in the vapor phase, water molecules colliding with the open end of the SWNT should be able to enter the channel more easily, hence maintain a higher concentration inside the SWNT than on the outside. Moreover, due to the one-dimensional confinement of the SWNT channel the water molecules inside it can form chain- or tubelike structures through hydrogen bonds,<sup>[16]</sup> and can be driven in a concerted fashion through application of an external field.<sup>[17]</sup>

Furthermore, we suggest that the coupling between water dipoles and free charge carriers of the nanotube is mutual, which – in conjunction with the concepts established above – clearly explains our experimental results: The electromotive force that is detected along the nanotube results from a directional flow of water inside the SWNT channel. The water itself is dragged by moving free charge carriers when an electric field is applied on the “motor” part (Fig. 1b). Since the experimental results presented in this paper are based on a metallic SWNT device, metallic SWNTs are discussed in detail in the following section. For a negative current (Fig. 2d), the water inside the “motor” part of the nanotube will be driven to flow from the “motor” part to the “generator” part. At the same time, electrons in the “generator” part of the SWNT will be dragged to move in the same direction resulting in their accumulation in the SWNT and generation of an electromotive force. This prevents further movement of electrons along the SWNT (Fig. 2d), hence a voltage difference can be detected between electrodes 1 and 2.<sup>[18]</sup> If the direction of the current is reversed (positive current), a voltage difference of opposite sign can be measured along the “generator” part. The absolute values of induced  $\Delta V$ s ( $|\Delta V|$ ) are almost equal for identical positive/negative currents (Figs. 2c and 3a). Notably, water molecules inside the “generator” part can be pushed (negative current) or pulled (positive current) by moving water molecules inside the “motor” part of the nanotube, and induce similar values of  $|\Delta V|$ . This indicates that the water molecules inside the SWNT are transported concertedly, as predicted previously.<sup>[2a,19]</sup>

Water molecules adsorbed on the outer surface of the nanotube may also be dragged by moving free charge carriers.

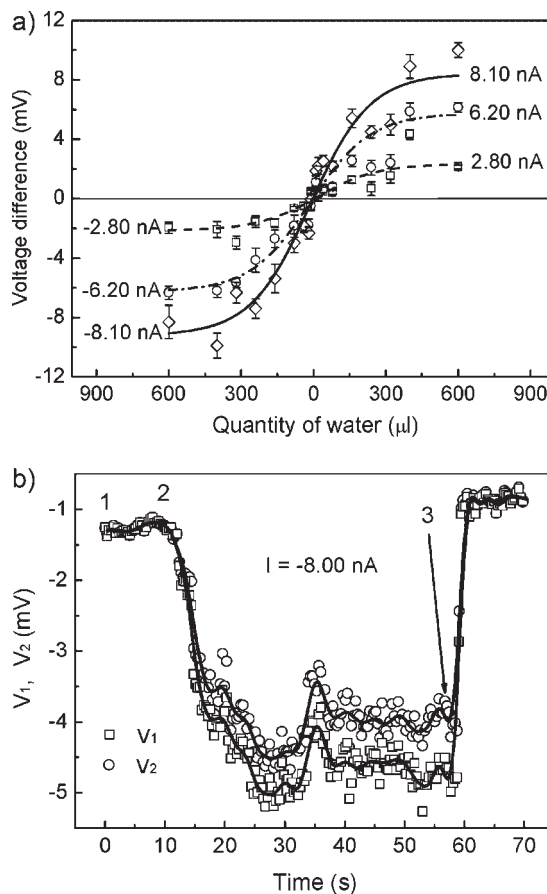


**Figure 3.** a) Dependence of the induced voltage difference on the quantity of water injected into the chamber. Induced  $\Delta V$  increases with the quantity of water inside the chamber and tends to saturate at  $\sim 500 \mu\text{L}$ . It is nearly symmetric for either a positive or negative current. b) Dynamic characteristics of the SWNT device when water is injected into or pumped out of the chamber.

However, they have no effect on the measurement results. In our experiments, the current flew along the “motor” part only, while no stable current was measured in other regions of the nanotube. We therefore conclude that only water molecules outside the “motor” part of the SWNT may obtain momentum. However, the nanotubes in our devices are in the contact regions entirely enclosed by metal electrodes (Fig. 1b), and it is feasible that the directional movement of outside water molecules from the “motor” part to the “generator” part could be blocked.

We have also investigated the dependence of the induced voltage difference on the quantity of water injected into the chamber. As shown in Figure 3a, the  $\Delta V$  that is induced increases linearly with the water quantity injected within a range of  $0\text{--}240 \mu\text{L}$ , and then, which is very interesting,  $\Delta V$  is gradually being saturated between  $240$  and  $500 \mu\text{L}$ . At constant current an increase in  $\Delta V$  can be attributed to an increase in the quantity of water inside the SWNT, which is caused by a higher concentration of water vapor in the chamber. However,  $\Delta V$

reaches saturation when the number of water molecules inside the SWNT reaches a maximum, even if the condensation of water molecules in the chamber is higher. This also indicates that the degree of filling of SWNTs has a maximum, i.e., SWNTs can be fully filled.

Figure 3b displays the dynamic characteristics of the device. The current applied to the “motor” part was set to  $-8.00\text{ nA}$  and at time point “2”  $60\text{ }\mu\text{L}$  water were injected into the evacuated chamber. Both,  $V_1$  and  $V_2$  decrease, and the voltage difference discussed earlier was observed. After  $\sim 15\text{ s}$  the voltage difference reached maximum and stabilized. The chamber was re-evacuated at time point “3”, upon which  $V_1$  and  $V_2$  were found to return to their original values in 2–3 s, which is much faster than the decreasing process for both,  $V_1$  and  $V_2$ . When the voltage difference reached its maximum and remained stable, an equilibrium state was attained for the flowing water molecules inside the SWNT, i.e., when some water molecules outflow at one end the same number of water molecules entered the nanotube from the other end. When the chamber is re-evacuated the number of water molecules in the chamber rapidly reduces and the equilibrium is disturbed. This causes the SWNT to be emptied very rapidly, and therefore  $V_1$  and  $V_2$  restore to their original values very quickly.

A similar voltage difference to the one discussed above was also detected in semiconducting SWNT devices (see Supporting Information, Fig. S3). However, the detected voltage difference is remarkably smaller than the observed in metallic SWNTs. This can be attributed to the much lower density of free charge carriers in semiconducting SWNTs. Furthermore, the  $I$ - $V$  characteristics of a device were measured in pure oxygen gas (see Supporting Information, Fig. S4), and no voltage difference was observed in the “generator” part. This indicates that the polar nature of water molecules is essential for the interaction between water molecules and nanotubes, which is in agreement with previously published works.<sup>[11,12]</sup>

In conclusion, a newly induced electromotive force was detected in the “generator” part of a water-filled SWNT when a current was applied on the “motor” part. We suggest that the water molecules inside the nanotube channel are dragged to flow directionally by an external electric field thereby generating an electromotive force along the nanotube. This energy conversion process is probably realized by the mutual coupling of water dipoles and free charge carriers present in SWNTs. Our results suggest that SWNTs can be exploited as unique, tunable molecular channels for water and might find potential application in nanoscale energy conversion. Nanofluidic logics based on the observed effects will also be of interest for future studies.

## Experimental

**Synthesis of Individual SWNTs:** Single-walled carbon nanotubes (SWNTs) were synthesized using floating catalytic chemical vapor deposition (CVD) [20]. The experimental setup consists of two tube furnaces: the first furnace is used for sublimation of the catalyst, while the second furnace is used for SWNT growth. An especially designed quartz tube is placed in the two furnace system. The main tube ( $\varnothing = 35\text{ mm}$ ) provides space for both, catalyst sublimation and SWNT growth, and between the two furnaces a transition tube ( $\varnothing = 10\text{ mm}$ ) is inserted into the main tube. A mixture of ferrocene and sulfur (molar ratio = 16: 1) served as catalyst source and was sublimed in the first furnace at a temperature of  $60\text{--}65\text{ }^\circ\text{C}$ , and subsequently carried through the transition tube into the second furnace by Ar ( $800\text{--}1200\text{ sccm}$ ) and methane ( $2\text{--}4\text{ sccm}$ ) flow. The reaction temperature of the second furnace was  $1100\text{ }^\circ\text{C}$ , and the pressure in the quartz tube was held constant at  $\sim 1\text{ atm}$ . Using these optimized parameters SWNTs were directly deposited onto various substrates. Most as-deposited SWNTs were isolated from each other. The average diameter of the obtained SWNTs is  $\sim 1.6\text{ nm}$ , which was determined by atomic force microscopy (see Supporting Information, Fig. S2).

**Fabrication of Suspended SWNT Devices:** Four steps were involved in the fabrication of suspended SWNT devices: Nitrogen-doped Si wafers (resistivity  $\sim 0.01\text{ }\Omega\text{ cm}^{-1}$ ) with a  $200\text{ nm}$  thick  $\text{SiO}_2$  surface layer were used as substrates and were firstly coated with a  $100\text{ nm}$  thick polymethylmethacrylate (PMMA) film. Then, individual SWNTs were deposited on the Si/SiO<sub>2</sub> substrates in the low temperature zone ( $<200\text{ }^\circ\text{C}$ ) of a floating catalytic chemical vapor deposition system (Fig. 4a) before another  $260\text{ nm}$  thick PMMA film was added on top of the as-deposited SWNTs (Fig. 4b). In a third step, desired patterns were defined in the PMMA film using electron beam lithography (EBL, Raith 150) and exposed PMMA was removed with a mixture of methyl isobutyl ketone (MIBK) and isopropyl alcohol. Ni/Au electrodes ( $20\text{ nm}/100\text{ nm}$ ) were then deposited at the desired positions via evaporation; and after lifting the devices off the wafer suspended SWNTs ( $\sim 100\text{ nm}$  above the substrate surface) were obtained (Fig. 4c). Finally, a focused ion beam (FIB, FEI, DB235) was used to open the nanotubes at both ends (Fig. 4d).

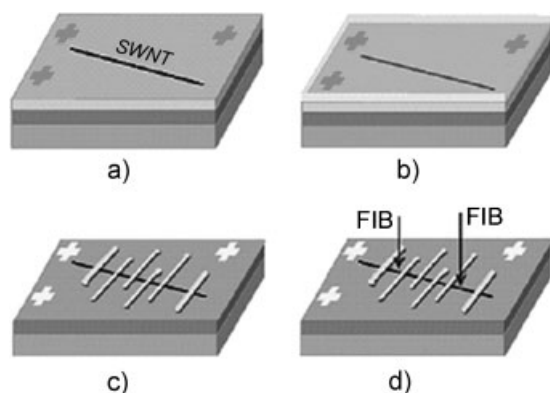


**Figure 4.** Fabrication process of suspended SWNT devices: a) Individual SWNTs are deposited on a Si/SiO<sub>2</sub> substrate covered with a  $100\text{ nm}$  thick polymethylmethacrylate (PMMA) film. b) Coating another layer of PMMA (thickness =  $260\text{ nm}$ ) on top of the SWNTs. c) Metal electrode (Ni/Au,  $120\text{ nm}$ ) fabrication. d) Opening the ends of suspended SWNTs via FIB.

Received: November 27, 2007

Revised: February 5, 2008

Published online:

- [1] a) L. D. Gelb, K. E. Gubbins, R. Radhakrishnan, B. M. Sliwinski, *Rep. Prog. Phys.* **1999**, *62*, 1573. b) M. Whitby, N. Quirke, *Nat. Nanotechnol.* **2007**, *2*, 87.

- [2] a) G. Hummer, J. C. Rasaiah, J. P. Noworyta, *Nature* **2001**, *414*, 188. b) K. Koga, G. T. Gao, H. Tanaka, X. C. Zeng, *Nature* **2001**, *412*, 802. c) A. Berezhevskii, G. Hummer, *Phys. Rev. Lett.* **2002**, *89*, 064503. d) Y. C. Liu, Q. Wang, *Phys. Rev. B* **2005**, *72*, 085420.
- [3] Y. Maniwa, H. Kataura, M. Abe, E. Udaka, S. Suzuki, Y. Achiba, H. Kira, K. Matsuda, H. Kadozaki, Y. Okabe, *Chem. Phys. Lett.* **2005**, *401*, 534.
- [4] a) S. Ghosh, K. V. Ramanathan, A. K. Sood, *Europhys. Lett.* **2004**, *65*, 678. b) K. Matsuda, T. Hibi, H. Kadowaki, H. Kataura, Y. Maniwa, *Phys. Rev. B* **2006**, *74*, 073415. c) S. H. Mao, A. Kleinhammes, Y. Wu, *Chem. Phys. Lett.* **2006**, *421*, 513.
- [5] a) A. I. Kolesnikov, J.-M. Zanotti, C.-K. Loong, P. Thiyagarajan, A. P. Moravsky, R. O. Loutfy, C. J. Burnham, *Phys. Rev. Lett.* **2004**, *93*, 035503. b) N. R. de Souza, A. I. Kolesnikov, D. J. Burnham, C.-K. Loong, *J. Phys.: Condens. Matter* **2006**, *18*, S2321.
- [6] O. Byl, J.-C. Liu, Y. Wang, W.-L. Yim, J. K. Johnson, J. T. Yates, *J. Am. Chem. Soc.* **2006**, *128*, 12090.
- [7] W. Wenseleers, S. Cambré, J. Čulin, A. Bouwen, E. Goovaerts, *Adv. Mater.* **2007**, *19*, 2274.
- [8] N. Naguib, H. H. Ye, Y. Gogotsi, A. G. Yazicioglu, C. M. Megaridis, M. Yoshimura, *Nano Lett.* **2004**, *4*, 2237.
- [9] a) M. Majumder, N. Chopra, R. Andrews, B. J. Hinds, *Nature* **2005**, *438*, 44. b) J. K. Holt, H. G. Park, Y. Wang, M. Stadermann, A. B. Artyukhin, C. P. Grigoropoulos, A. Noy, O. Bakajin, *Science* **2006**, *312*, 1034.
- [10] Y. Maniwa, K. Matsuda, H. Kyakuno, S. Ogasawara, T. Hibi, H. Kadowaki, S. Suzuki, Y. Achiba, H. Kataura, *Nat. Mater.* **2007**, *6*, 135.
- [11] a) A. Maiti, J. Andzelm, N. Tanpipat, P. von Allmen, *Phys. Rev. Lett.* **2001**, *87*, 155502. b) J. J. Zhao, A. Buldum, J. Han, J. P. Lu, *Nanotechnology* **2002**, *13*, 195. c) D. Y. Lu, Y. Li, S. V. Rotkin, U. Ravaioli, K. Schulten, *Nano Lett.* **2004**, *4*, 2383.
- [12] a) S. Ghosh, A. K. Sood, N. Kumar, *Science* **2003**, *299*, 1042. b) S. Ghosh, A. K. Sood, S. Ramaswamy, N. Kumar, *Phys. Rev. B* **2004**, *70*, 205423.
- [13] P. Král, M. Shapiro, *Phys. Rev. Lett.* **2001**, *86*, 131.
- [14] S. Heinze, J. Tersoff, R. Martel, V. Derycke, J. Appenzeller, Ph. Avouris, *Phys. Rev. Lett.* **2002**, *89*, 106801.
- [15] a) A. Zahab, L. Spina, P. Poncharal, C. Marlière, *Phys. Rev. B* **2000**, *62*, 10000. b) P. S. Na, H. J. Kim, H. M. So, K. J. Kong, H. J. Chang, B. H. Ryu, Y. M. Choi, J. O. Lee, B. K. Kim, J. J. Kim, *Appl. Phys. Lett.* **2005**, *87*, 093101.
- [16] a) W. H. Noon, K. D. Ausman, R. E. Smalley, J. P. Ma, *Chem. Phys. Lett.* **2002**, *355*, 445. b) R. J. Mash, S. Joseph, N. R. Aluru, E. Jakobsson, *Nano Lett.* **2003**, *3*, 589. c) S. Vaitheeswaran, J. C. Rasaiah, G. Hummer, *J. Chem. Phys.* **2004**, *121*, 7955.
- [17] a) X. J. Gong, J. Y. Li, H. J. Lu, R. Z. Wan, J. C. Li, J. Hu, H. P. Fang, *Nat. Nanotechnol.* **2007**, *2*, 709. b) J. Y. Li, X. J. Gong, H. J. Lu, D. Li, H. P. Fang, R. H. Zhou, *Proc. Natl. Acad. Sci. USA* **2007**, *104*, 3687.
- [18] J. Yang, F. Lu, L. W. Kostiuk, D. Y. Kwok, *J. Micromech. Microeng.* **2003**, *13*, 963.
- [19] a) A. Striolo, *Nano Lett.* **2006**, *6*, 633. b) E. M. Kotsalis, J. H. Walther, P. Koumoutsakos, *Int. J. Multiphase Flow* **2004**, *30*, 995.
- [20] a) L. Song, L. J. Ci, L. Lv, Z. P. Zhou, X. Q. Yan, D. F. Liu, H. J. Yuan, Y. Gao, J. X. Wang, L. F. Liu, X. W. Zhao, Z. X. Zhang, X. Y. Dou, W. Y. Zhou, G. Wang, C. Y. Wang, S. S. Xie, *Adv. Mater.* **2004**, *16*, 1529. b) Z. P. Zhou, L. J. Ci, L. Song, X. Q. Yan, D. F. Liu, H. J. Yuan, Y. Gao, J. X. Wang, L. F. Liu, W. Y. Zhou, G. Wang, S. S. Xie, *J. Phys. Chem. B* **2004**, *108*, 10751.